COLLOQUIA: LaThuile11

CP violation and rare B_s decays at the Tevatron

M. D. CORCORAN for the CDF and D0 COLLABORATIONS

Rice University, USA

Summary. — This note gives updates on three results from the Fermilab Tevatron $p\bar{p}$ collider operating at $\sqrt{s} = 1.96$ TeV. The results presented include: the D0 dimuon charge asymmetry; the measurement of the CP-violating phase ϕ_s in the decay $B_s \to J/\psi\phi$ from both CDF and D0; and the most recent results from both CDF and D0 on the search for the ultra-rare decay $B_s \to \mu^+\mu^-$.

PACS 11.30.Er – Charge conjugation, parity, time reversal, and other discrete symmetries.
PACS 13.20.He – Leptonic, semileptonic, and radiative decays of mesons: Decays of bottom mesons.
PACS 13.25.Hw – Hadronic decays of mesons: Decays of bottom mesons.

1. – Introduction

CP violation was first observed in the $K^0/\overline{K^0}$ system in 1964 [1]. In 1967 Andrei Sakharov showed that CP violation is a necessary ingredient in the generation of the matter-antimatter asymmetry of the universe [2]. In the standard model (SM), CP violation arises from the complex phase in the CKM matrix, but the amount of CP violation from this source is too small by many orders of magnitude to account for the observed asymmetry. So we have a long-standing puzzle as to the origin of the missing CP violation.

Neutral mesons such as K^0, D^0, B_d^0 and B_s^0 can mix through double W-exchange (the "box diagram"), as shown in fig. 1. Asymmetric mixing , which is both CP and T violating, occurs when the rate of (for example) $B_s \to \overline{B_s}$ is not equal to the rate $\overline{B_s} \to B_s$. The solution to the time-dependent Schroedinger equation in this case yields two mass eigenstates which are not CP eigenstates and which have different masses (usually referred to as "heavy" and "light") and different lifetimes. CP violation can also arise from interference of the decay and mixing amplitudes through phases, or directly through the decay amplitudes.

The neutral Kaon system has been well studied for many years, and the B_d system has been extensively studied at the B-factories, resulting in stringent constraints on the
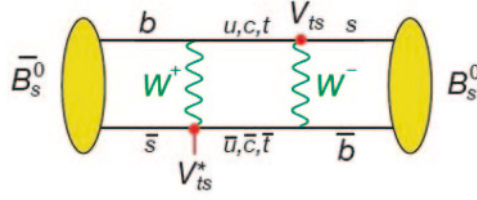
Fig. 1. – Box diagram for B_s mixing.

CKM matrix elements and therefore on CP-violating parameters in the B_s system. Any deviation from the SM expectations would be an indication of new physics.

The physics parameters related to B_s mixing are: Δm_s, the mass difference between the light and heavy eigenstates (well-measured by CDF to be $17.77 \pm 0.12 \, \mathrm{ps}^{-1}$ [3]); $\Delta\Gamma$, the lifetime difference between the light and heavy eigenstates; and ϕ_s, the phase between the decay and mixing amplitudes. The SM expectation for $\Delta\Gamma$ is 0.096 ± 0.0014, and the SM expectation for ϕ_s is 0.0042 ± 0.0014. The small expected value of ϕ_s makes its measurement especially interesting in the search for new physics. One can write $\phi_s = \phi_s^{SM} + \phi_s^{NP}$, where SM refers to the standard model contribution, and NP refers to a possible new phenomena contribution.

The decay $B_s \to J/\psi\phi$ can occur directly, or the B_s meson could first mix and then decay: $B_s \to \overline{B_s} \to J/\psi\phi$. Interference between these two processes is characterized by the phase β_s which in the SM is related to the CKM matrix elements by $\beta_s^{SM} = arg[-V_{ts}V_{tb}^*/V_{cs}V_{cb}^*]$. The SM expectation for this quantity is small, with $\beta_s^{SM} = 0.038 \pm 0.002$. Note that D0 uses the quantity $\phi_s^{J/\psi\phi} = -2\beta_s$. If new physics enters B_s mixing and $B_s \to J/\psi\phi$ the same way, we would have $\phi_s^{J/\psi\phi} = -2\beta_s + \phi_s^{NP}$, with ϕ_s^{NP} the same for B_s mixing and for $B_s \to J/\psi\phi$.

Decays which are heavily suppressed in the SM are another excellent place to search for new physics. The decay $B_s \to \mu\mu$ is highly suppressed in the SM since it is a flavor changing neutral current which is also helicity suppressed. Many scenarios of physics beyond the SM, in particular Supersymmetry, produce enhancements of this process by large factors, which makes this rare decay a promising place to search for new processes.

2. – Dimuon charge asymmetry

The D0 collaboration has measured the like-sign dimuon charge asymmetry from B decays, defined as

$$A_{sl}^b = \frac{N_b^{++} - N_b^{--}}{N_b^{++} + N_b^{--}},$$

where $N_b^{++}(N^{--})$ refers to the number of events from $B/\overline{B}$ meson decays with two positive (negative) muons. $B/\overline{B}$ meson decays can lead to muons of the same charge if one of the mesons mixes and they both undergo semileptonic decays to muons. Only if the rate of $B \to \overline{B}$ is not equal to the rate of $\overline{B} \to B$ will A_{sl}^b be nonzero. Therefore this asymmetry directly measures CP-violating effects. The SM expectation for this quantity is $A_{sl}^b(SM) = (-2.8^{+0.5}_{-0.6}) \times 10^{-4}$, below the sensitivity of the D0 experiment.
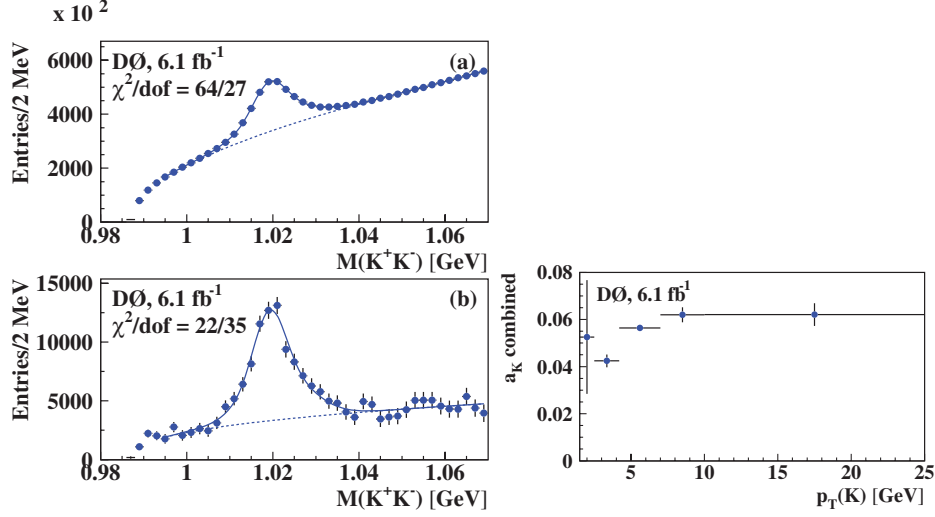
Fig. 2. – K^+K^- mass distributions. (a) The sum of $K^+ \to \mu^+$ and $K^- \to \mu^-$, with the ϕ peak clearly visible. (b) The difference $K^+ \to \mu^+ - K^- \to \mu^-$. The excess of positive muons is due to the larger interaction cross section for K^-, resulting in an overall charge asymmetry. The right plot shows the combined K asymmetry as determined from $\phi \to KK$ and $K^{0*} \to K\pi$ decays.

D0 also measures the single-muon charge asymmetry a_{sl}^b, defined as

$$a_{sl}^b = \frac{\Gamma(\overline{B} \to \mu^+ X) - \Gamma(B \to \mu^- X)}{\Gamma(\overline{B} \to \mu^+ X) + \Gamma(B \to \mu^- X)} \,,$$

which can be shown to be equal to A_{sl}^b. There are thus two independent measurements of the same quantity. The final result will take advantage of the fact that many of the systematic errors of these two measurements are highly correlated, allowing some cancellation.

In this measurement, no distinction is made between B_d and B_s mesons, so the measured quantity is a linear combination of the asymmetries from B_d (a_{sl}^d) and B_s (a_{sl}^s). The coefficients of the linear combination are known from other measurements at B factories and at the Tevatron. The analysis selects well-identified muons to define the inclusive muon sample (1.5×10^9 events) and the like-sign dimuon sample (3.7×10^6 events). The data sample corresponds to $6.1\,\text{fb}^{-1}$ of recorded luminosity.

After initial selection, corrections are made for backgrounds from hadrons that fake muons and for detector-related asymmetries. These corrections are determined almost completely from the data. Then corrections are made for non-B contributions and non-oscillating contributions to the inclusive and dimuon samples. The final step uses the two independent measurements of A_{sl}^b to cancel some systematics.

The most significant source of background is due to $K \to \mu\nu$ decays which have an asymmetry due to the larger cross section for K^- interactions in matter compared to K^+. Processes such as $K^- p \to \Lambda\pi^0$ are possible for the K^- but not K^+. Therefore more K^- mesons interact with the detector material and do not survive long enough to decay, leading to a significant positive charge asymmetry that must be measured and corrected for. This background is measured from the data in two ways: from $\phi \to KK$ and from
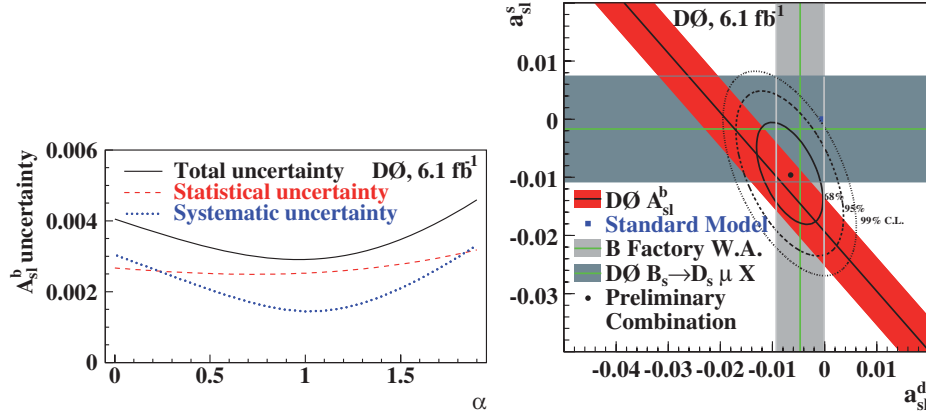
Fig. 3. – The left plot shows the error on A_{sl}^b as a function of the combination parameter α. The value of α is chosen to minimize the overall error. The right figure shows the two-dimensional plot of the semileptonic charge asymmetries a_{sl}^d *vs.* a_{sl}^s. The diagonal band is the result of this measurement. The vertical band is the world average measurement of a_{sl}^d from B-factories. The horizontal band is an independent measurement of a_{sl}^s from D0. The solid circle is the combination of these three measurements, and the square point is the SM expectation.

$K^{0*} \to K\pi$. Figure 2 shows the $\phi \to KK$ signal for events in which one of the K's has faked a muon. The top-left plot (a) shows the sum of positive and negative muons, while the bottom-left plot (b) shows the difference of positive and negative muons. There is a significant asymmetry as expected. The K asymmetry is also measured using $K^* \to K\pi$, yielding consistent results. The right plot in fig. 2 shows the overall K asymmetry as determined from both decay modes. There are also fake muons from π decay and proton punchthrough. These asymmetries are measured using $K_s \to \pi\pi$ and $\Lambda \to p\pi$ and are much smaller than the K asymmetry.

In addition to the asymmetry from $K \to \mu$ decays, the fraction of muons due to K decay must be determined. This fraction is determined from the data using K^* decays. Then Monte Carlo ratios of K/π and K/p are used to determine the π and proton fraction of fake muons.

An important feature of the D0 detector is the periodic changing of the magnet polarities for both the solenoid and toroid. Detector-related asymmetries are nearly completely canceled out when the different magnet polarities are combined. Any residual asymmetries are measured from $J/\psi \to \mu\mu$ decays and corrected for.

The final result is obtained by combining the uncorrected asymmetries A (from the dimuon sample) and a (from the inclusive muon sample) $A' = A - \alpha a$, where α is a parameter which is varied to minimize the final error. Figure 3 shows the total uncertainty as a function of the parameter α. The result is $A_{sl}^b = [-0.957 \pm 0.251 (\text{stat}) \pm 0.146 (\text{syst})]\%$ while the SM expectation is $A_{sl}^b (SM) = [0.023^{+0.005}_{-0.006}]\%$. Figure 3 also shows the final result plotted in the a_{sl}^d *vs.* a_{sl}^s plane along with the world average results for a_{sl}^d from the B factories and a_{sl}^s from the D0 measurement of $B_s \to D_s\mu X$. The SM expectation is shown as the square point, and the solid dot is the combination of the three measurements. This result has a 3.2 standard deviation discrepancy with the SM expectation. Many cross checks have been carried out and are detailed in the publications [4]. An update of this result with more data, improved background determinations, and varying impact parameter bins is underway.
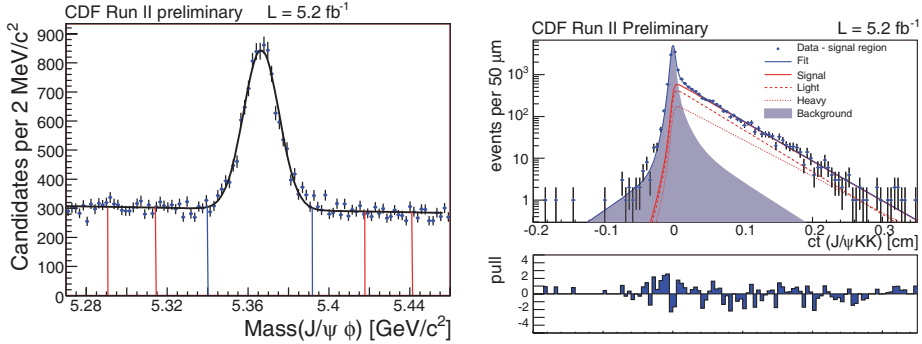
Fig. 4. – The left plot shows the $\mu\mu KK$ mass distribution for events entering into the fit. The right plot shows the lifetime distribution.

3. – $B_s \to J/\psi\phi$

The decay $B_s \to J/\psi\phi$ is of special interest since previously a CDF/D0 combination showed a 2.1 σ discrepancy with the SM for the phase $\phi_s^{J/\psi\phi} \approx -2\beta_s$ [5]. CDF and D0 both have recent updates to this analysis. This decay is complicated since it is a scalar meson decaying into two vector particles. The final state particles are detected in the decays $J/\psi \to \mu\mu$ and $\phi \to KK$. The relative orbital angular momentum of the J/ψ and ϕ can take on values $l = 0, 1, 2$, and therefore decay is described by three complex amplitudes. The fits to the lifetime distributions require of order 30 parameters including background, so care must be taken to ensure stability. Both experiments do unbinned maximum-likelihood fits. The recent CDF result [6] is based on $5.2\,\mathrm{fb}^{-1}$ of integrated luminosity. Figure 4 shows the mass and lifetime distributions for events entering into the fit. As can be seen in the figure, the fit includes both heavy and light eigenstates with different lifetimes. The two-dimensional likelihood contours of the phase β_s *vs.* the lifetime difference between the two mass eigenstates, $\Delta\Gamma$, are shown in fig. 5 along with
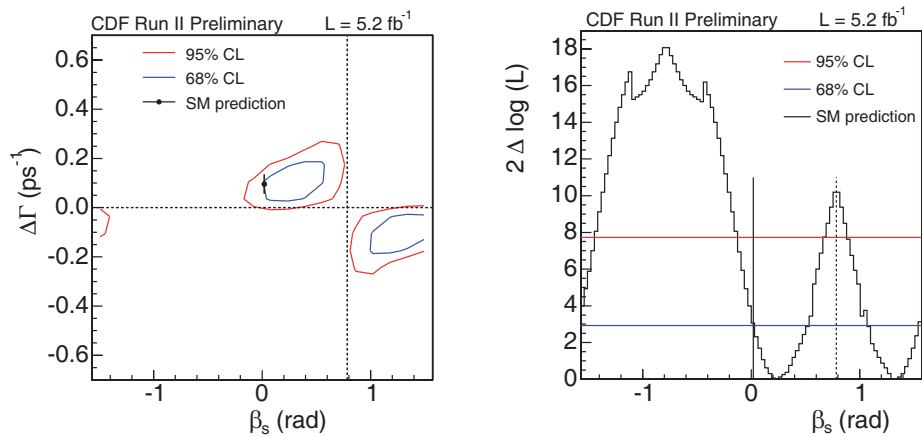

Fig. 5. – The left plot shows the CDF two-dimensional plot of the 68% and 95% confidence level contours in the β_s *vs.* $\Delta\Gamma$ plane. The right plot shows the one-dimensional projection of β_s.
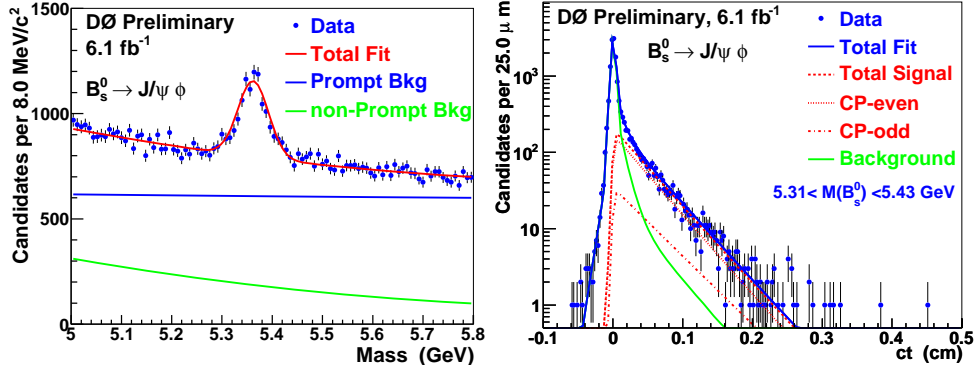
Fig. 6. – D0 mass and lifetime distributions for $B_s \to J/\psi\phi$.

the one-dimensional projection of β_s. The SM expectation is shown as the black point. The CDF result agrees with the SM within one standard deviation.

D0 also has presented a new preliminary result for this decay mode [7]. The analysis technique is similar to CDF's, with a maximum-likelihood fit being done to about 30 parameters. Figure 6 shows the D0 mass and lifetime distributions with the fit results. The D0 fits have constrained the strong phases δ_1 and δ_2 to values near the $B^0 \to J/\psi K^*$ values measured by B-factories. Gronau and Rosner [8] have argued that the strong phases should be similar for B_s and B_d decays. The D0 result for the two-dimensional likelihood contours for $\phi_s^{J/\psi\phi}$ vs. $\Delta\Gamma$ and the one-dimensional projection for $\phi_s^{J/\psi\phi}$ are shown in fig. 7. The 68% and 95% CL bands from the same-sign dimuon charge asymmetry result are shown in the left plot. The D0 one-dimensional projection deviates from the SM value by about two standard deviations. The situation therefore remains somewhat murky, with CDF's most recent result in agreement with the SM, while the D0 result still deviates from the SM by about the same amount as the earlier result. Both experiments agree that there can be significant variation of results from experiment to experiment, or for different subsets of the data within the same experiment. For
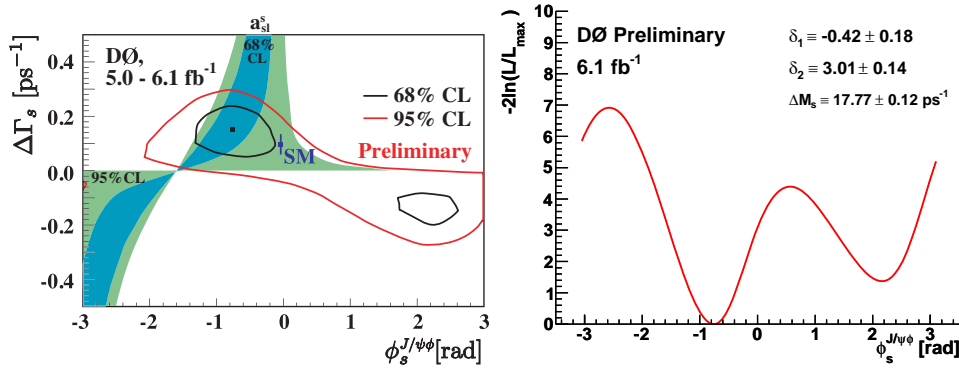

Fig. 7. – D0 likelihood contours for $\phi_s^{J/\psi\phi}$ vs. $\Delta\Gamma$(left). The 68% and 95% CL bands from the dimuon charge asymmetry result are also shown. The right plot shows the one-dimensional projection of $\phi_s^{J/\psi\phi}$.
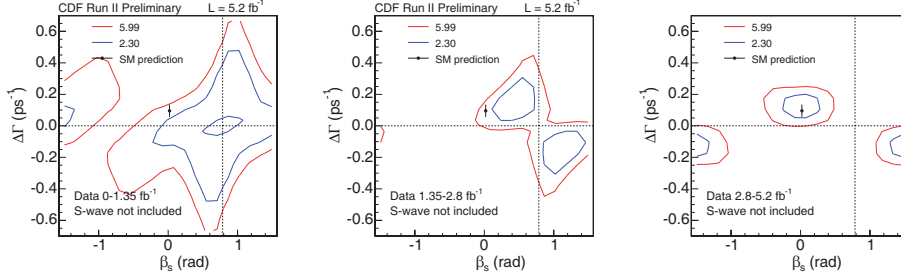
Fig. 8. – CDF likelihood contours for three different data-taking periods.

example, fig. 8 shows CDF results divided into three data-taking periods of about the same integrated luminosity. Although the detector and analysis techniques are the same, the results vary significantly for the three periods. Both CDF and D0 are working on further updates of this analysis.

4. – $B_s \to \mu^+\mu^-$

The SM expected branching ratio is $(3.6 \pm 0.3) \times 10^{-9}$ [9]. The most recent CDF branching ratio limit [10] at the 95% CL is 43×10^{-9} (33×10^{-9}) for the observed (expected) limit.

D0 has a recent update on this measurement [11] based on $6.1\,\mathrm{fb}^{-1}$ of recorded luminosity. The analysis uses a Baysian neural network (BNN) with six variables to separate signal from background. The variables that were found to have the best signal/background separation power were: the minimum muon impact parameter; dimuon
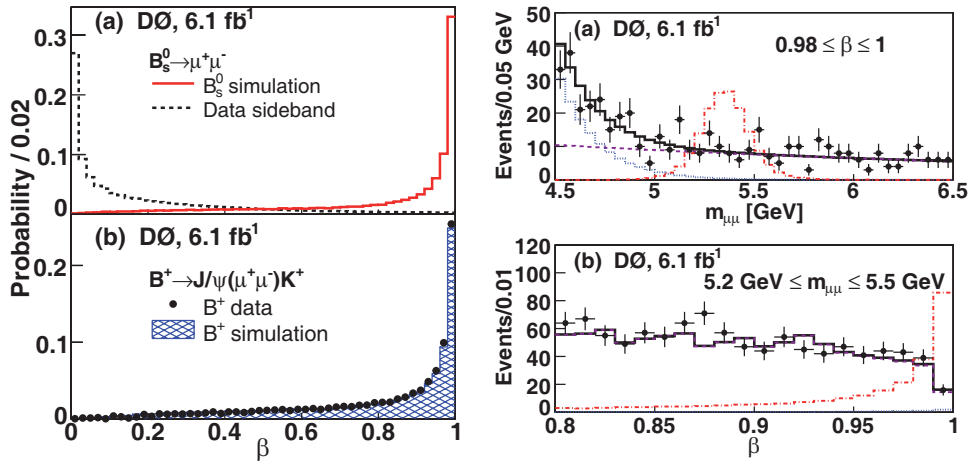

Fig. 9. – D0 search for $B_s \to \mu\mu$. The top left plot shows the output of the BNN for signal Monte Carlo and data sideband backgrounds. The bottom left shows the BNN output for the normalization mode. The right plot shows the projections of the dimuon mass and BNN output parameter β for the most sensitive bin of BNN output. The dot-dash curve shows a simulated signal at $100\times$ the SM expectation.

vertex χ^2; the decay length significance; the angle between the dimuon momentum vector and the vector from the primary vertex to the secondary vertex (the "pointing angle"); and the minimum muon transverse momentum. Monte Carlo studies indicate that the most serious background is due to production of a $b\bar{b}$ pair, both of with decay semileptonically. Signal Monte Carlo and data sidebands are used to train the BNN. Figure 9 shows the output of the BNN for signal Monte Carlo and data sidebands. This figure also shows the selection for the normalization mode $B^{\pm} \to J/\psi K^{\pm}$. The final limit is calculated in bins of $\mu\mu$ mass and β, the output of the BNN. Figure 9 shows the projection in dimuon mass and β for the most sensitive bin in β. The dot-dashed curve represents a signal $100\times$ the SM expectation. There is no evidence of a signal, and D0 sets a branching ratio limit at the 95% CL of 51×10^{-9} (38×10^{-9}) for the observed (expected) limit. Both experiments are working on an update to this measurement.

5. – Conclusion

The D0 like-sign dimuon charge asymmetry exhibits a 3.2 σ discrepancy with the SM. An update on this result, including an impact parameter study and more data, should be available soon. This result challenges the SM, and it is important to have this result verified (or not) by another experiment.

The decay $B_s \to J/\psi\phi$ has been studied by both CDF and D0. Extracting the physics parameters requires a complicated fit of 30+ parameters. The current situation is unclear, with CDF's most recent result in agreement with the SM, and D0's result still about two standard deviations away from the SM expectation. But within errors the two experiments are in agreement.

Both CDF and D0 have presented branching ratio limits for the ultra-rare decay $B_s \to \mu\mu$ which are about 10 times the SM expectation. Both CDF and D0 are continuing to push the branching ratio limits on this mode.

REFERENCES

[1] Christiansen J. H., Cronin J. W., Fitch V. L. and Turlay R., *Phys. Rev. Lett.*, **13** (1964) 138.
[2] Sakharov A. D., *JETP*, **5** (1967) 24.
[3] Abulencia A. *et al.*, *Phys. Rev. Lett.*, **97** (2006) 242003.
[4] Abazov V. *et al.*, *Phys. Rev. D*, **82** (2010) 032001; Abaov V. *et al.*, *Phys. Rev. Lett.*, **105** (2010) 081801.
[5] CDF and D0 Collaborations, Combination of D0 and CDF Results on $\Delta\Gamma$ and the CP-Violating Phase $\beta_s^{J/\psi\phi}$, CDF/PHYS/BOTTOM/CDFR/9787 and D0 Note 5928-CONF, 2009.
[6] CDF Collaboration, "An Updated Measurement of the CP Violating Phase $\beta_s^{J/\psi\phi}$ in $B_s^0 \to J/\psi\phi$ Decays using $5.2\,\mathrm{fb}^{-1}$ of Integrated Luminosity", CDF/ANAL/BOTTOM/PUBLIC/10206 (2010).
[7] D0 Collaboration, "Updated Measurement of the CP-Violating Phase $\phi_s^{J/\psi\phi}$ Using the Flavor-tagged Decay $B_s \to J/\psi\phi$, D0 Note 6098-CONF (2010).
[8] Gronau M. and Rosner J. L., *Phys. Lett. B*, **669** (2008) 321.
[9] Buras A. J., *Prog. Theor. Phys*, **122** (2009) 145.
[10] CDF Collaboration, "Search for $B_s^0 \to \mu^+\mu^-$ and $B_d^0 \to \mu^+\mu^-$ Decays on $3.7\,\mathrm{fb}^{-1}$ of $p\bar{p}$ Collisions with CDF II", CDF Public Note 9892.
[11] Abazov V. *et al.*, *Phys. Lett. B*, **693** (2010) 539.